International Journal of Fracture **63**: 229–245, 1993.

Numerical solutions of singular integral equations having Cauchy-type singular kernel by means of expansion method

NAO-AKI NODA and TADATOSHI MATSUO
Department of Mechanical Engineering, Kyushu Institute of Technology, Kitakyushu 804, Japan

Received 5 January 1993; accepted in revised form 4 August 1993

Abstract. This paper is concerned with numerical solutions of singular integral equations with Cauchy-type singular kernel. It is well-known that this type of singular integral equations appears in the analysis of crack problems using the continuously distributed dislocation method. In addition, it also appears in the analysis of notch problems using the body force method. In the present analysis, the unknown function of densities of dislocations and body forces are approximated by the product of the fundamental density functions and polynomials. The accuracy of stress intensity factors and stress concentration factors obtained by the present method is verified through the comparison with the exact solution and the reliable numerical solution obtained by other researchers. The present method is found to give good convergency of the numerical results for notch problem as well as internal and edge crack problems.

1. Introduction

In the analysis of stress intensity factors for crack problems, various numerical methods, such as conformal mapping technique, Laurent series expansion method, body force method, continuously distributed dislocation method and finite element method have been applied to different types of problems depending on their peculiarity. Among those methods, the continuously distributed dislocation method has been used by a lot of researchers: in the analysis, a crack is represented by a distribution of infinitesimal dislocations and the problem is reduced to the singular integral equations having Cauchy-type singular kernel. To solve this type of singular integral equations, Erdogan [1, 2], Theocaris-Ioakimidis [3], Boiko-Kerpenko [4] and other researchers have discussed several numerical methods. Recently, Fujimoto [5] has applied Boiko's method to internal crack problems and has shown that internal crack problems are solved with higher accuracy than previous research has shown.

On the other hand, in previous papers [6, 7, 8], numerical solutions of the singular integral equation in the crack analysis using the body force method, which has the singularity of the form r^{-2}, have been discussed. Then, an approximation of the unknown function by the product of the fundamental density function and Chebyshev polynomials is found to give more accurate results compared with previous research. In this paper, the Cauchy-type singular integral equations for crack and notch problems are solved using a similar approximation, namely, by the product of the fundamental density function and polynomials. Then, the accuracy of stress intensity factors obtained by the present method are compared with the results given by the hypersingular integral equations in the previous paper. Moreover, problems of a cruciform crack, an internal crack and an edge crack are solved and compared with exact solutions and reliable numerical solutions obtained by quadrature methods. The problem of a semi-elliptical notch is also solved and the results are compared with previous body force method research [9, 10].

2. Numerical solution of singular integral equations using expansion method

In this section, the present numerical solution is described for internal crack problem, edge crack problem and notch problem, separately.

2.1. Numerical solution for internal crack problem

Consider a two-dimensional elastic plate with a straight crack whose length is $(b - a)$. This problem may be reduced to the following integral equations where two kinds of dislocation densities, tension and shear type $P_1(\xi)$ and $P_2(\xi)$, at the imaginary crack surface are to be unknown functions

$$\begin{aligned} &\oint_a^b \frac{P_1(\xi)}{\xi - x}\,\mathrm{d}\xi + \int_a^b K_{11}(\xi, x)P_1(\xi)\,\mathrm{d}\xi + \int_a^b K_{12}(\xi, x)P_2(\xi)\,\mathrm{d}\xi = -\frac{1+\kappa}{2G}p(x). \\ &\oint_a^b \frac{P_2(\xi)}{\xi - x}\,\mathrm{d}\xi + \int_a^b K_{21}(\xi, x)P_1(\xi)\,\mathrm{d}\xi + \int_a^b K_{22}(\xi, x)P_2(\xi)\,\mathrm{d}\xi = -\frac{1+\kappa}{2G}q(x). \end{aligned} \tag{1}$$

$$\int_a^b P_1(\xi)\,\mathrm{d}\xi = 0, \quad \int_a^b P_2(\xi)\,\mathrm{d}\xi = 0, \tag{2}$$

where $\kappa = 3 - 4\nu$ (for plane strain), G is shear modulus and ν is Poisson's ratio. Here $\oint$ is interpreted in the sense of Cauchy's principle of integration and the kernel $K_{ij}(\xi, x)$ $(i, j = 1, 2)$ is a function known to satisfy the boundary condition except at the crack surface. And $p(x)$, $q(x)$ are normal and shear traction prescribed on the crack surface. Equations (2) are additional conditions which mean the total sum of dislocation densities should be zero because of the single-valuedness of displacement.

First, normalizing the interval (a, b) of integration by defining

$$r = \frac{2\xi - (a - b)}{b - a}, \quad s = \frac{2x - (a + b)}{b - a}, \tag{3}$$

$$f_i(r) = \frac{2P_i(\xi)}{b - a}, \quad (i = 1, 2). \tag{4}$$

The integral equations (1), (2) become

$$\begin{aligned}
&\int_{-1}^{1} \frac{f_1(r)}{r-s}\,\mathrm{d}r + \int_{-1}^{1} k_{11}(r,s)f_1(r)\,\mathrm{d}r + \int_{-1}^{1} k_{12}(r,s)f_2(r)\,\mathrm{d}r = -\frac{1+\kappa}{2G}p(s),\\
&\int_{-1}^{1} \frac{f_2(r)}{r-s}\,\mathrm{d}r + \int_{-1}^{1} k_{21}(r,s)f_1(r)\,\mathrm{d}r + \int_{-1}^{1} k_{22}(r,s)f_2(r)\,\mathrm{d}r = -\frac{1+\kappa}{2G}q(s),
\end{aligned} \tag{5}$$

$$\int_{-1}^{1} f_1(r)\,\mathrm{d}r = 0, \quad \int_{-1}^{1} f_2(r)\,\mathrm{d}r = 0. \tag{6}$$

In the solution of (5), the unknown function $f_i(r)$ $(i = 1, 2)$ is approximated by the product of the fundamental dislocation density function $w_i(r)$ $(i = 1, 2)$ and Chebyshev polynomial $T_n(r)$

$$W_i(r) = \frac{1+\kappa}{2G\sqrt{1-r^2}}, \quad (i = 1, 2), \tag{7}$$

$$\begin{aligned}
&f_1(r) = W_1(r)F_{\mathrm{I}}(r), \quad F_{\mathrm{I}}(r) = \sum_{n=1}^{N} a_n T_n(r),\\
&f_2(r) = W_2(r)F_{\mathrm{II}}(r), \quad F_{\mathrm{II}}(r) = \sum_{n=1}^{N} b_n T_n(r).
\end{aligned} \tag{8}$$

The integral involves a singular term which is evaluated by using the following expression

$$\int_{-1}^{1} \frac{T_n(r)}{(r-s)\sqrt{1-r^2}}\,\mathrm{d}r = \pi U_{n-1}(s) \tag{9}$$

where $T_n(r)$ and $U_n(r)$ are the first and the second kind of Chebyshev polynomials, respectively, and are represented by the following expression

$$T_n(r) = \cos(n\theta), \quad U_{n-1}(r) = \frac{\sin(n\theta)}{\sin\theta}, \quad r = \cos\theta. \tag{10}$$

By substituting from (7) and (8) into (5) and using (9), the following set of $2N$ linear equations is obtained

$$\begin{aligned}
&\sum_{n=1}^{N} [a_n\{\pi U_{n-1}(s) + A_n(s)\} + b_n B_n(s)] = -\pi p(s),\\
&\sum_{n=1}^{N} [\mathrm{a}_n \mathrm{C}_n(\mathrm{s}) + \mathrm{b}_n\{\pi U_{n-1}(s) + D_n(s)\}] = -\pi q(s),
\end{aligned} \tag{11}$$

where

$$A_n(s) = \int_{-1}^{1} k_{11}(r, s) \frac{T_n(r)}{\sqrt{1 - r^2}} \mathrm{d}r,$$

$$B_n(s) = \int_{-1}^{1} k_{12}(r, s) \frac{T_n(r)}{\sqrt{1 - r^2}} \mathrm{d}r,$$

$$C_n(s) = \int_{-1}^{1} k_{21}(r, s) \frac{T_n(r)}{\sqrt{1 - r^2}} \mathrm{d}r, \tag{12}$$

$$D_n(s) = \int_{-1}^{1} k_{22}(r, s) \frac{T_n(r)}{\sqrt{1 - r^2}} \mathrm{d}r.$$

The unknown coefficients a_n, b_n are determined from (11). And additional condition (6) is satisfied automatically by the method mentioned above. The convenient set of collocation points is given by

$$s = \cos\left(\frac{2j}{N + 1} \tfrac{1}{2}\pi\right), \quad j = 1, 2, \ldots, N \quad (-1 < s < 1). \tag{13}$$

The stress intensity factors can be calculated from

$$K_{\mathrm{IB}} = F_{\mathrm{IB}}(1)\sqrt{\pi(b - a)/2},$$

$$K_{\mathrm{IA}} = F_{\mathrm{IA}}(-1)\sqrt{\pi(b - a)/2},$$

$$K_{\mathrm{IIB}} = F_{\mathrm{IIB}}(1)\sqrt{\pi(b - a)/2}, \tag{14}$$

$$K_{\mathrm{IIA}} = F_{\mathrm{IIA}}(-1)\sqrt{\pi(b - a)/2}.$$

2.2. Numerical solution for edge crack problem

Consider an elastic plate with a straight edge crack whose length is a. This problem may be reduced to the following integral equations where the dislocation densities at the imaginary crack surface $P_1(\xi)$, $P_2(\xi)$ are to be unknown functions.

$$⨍_0^a \frac{P_1(\xi)}{\xi - x} \mathrm{d}\xi + \int_0^a K_{11}(\xi, x) P_1(\xi)\,\mathrm{d}\xi + \int_0^a K_{12}(\xi, x) P_2(\xi)\,\mathrm{d}\xi = -\frac{\kappa + 1}{2G} p(x),$$

$$⨍_0^a \frac{P_2(\xi)}{\xi - x} \mathrm{d}\xi + \int_0^a K_{21}(\xi, x) P_1(\xi)\,\mathrm{d}\xi + \int_0^a K_{22}(\xi, x) P_2(\xi)\,\mathrm{d}\xi = -\frac{\kappa + 1}{2G} q(x). \tag{15}$$

Normalizing the interval $(0, a)$ of integration by defining

$$r = \frac{\xi}{a}, \quad s = \frac{x}{a}, \tag{16}$$

$$f_i(r) = \frac{P_i(\xi)}{a}, \quad (i = 1, 2). \tag{17}$$

In order to use integration formula (9), Eqn. (15) is transformed to the following expression.

$$\begin{aligned} &\int_{-1}^{1} \frac{f_1(r)}{r-s}\,\mathrm{d}r - \int_{-1}^{0} \frac{f_1(r)}{r-s}\,\mathrm{d}r + \int_0^1 k_{11}(r,s) f_1(r)\,\mathrm{d}r + \int_0^1 k_{12}(r,s) f_2(r)\,\mathrm{d}r = -\frac{\kappa+1}{2G}p(s), \\ &\int_{-1}^{1} \frac{f_2(r)}{r-s}\,\mathrm{d}r - \int_{-1}^{0} \frac{f_2(r)}{r-s}\,\mathrm{d}r + \int_0^1 k_{21}(r,s) f_1(r)\,\mathrm{d}r + \int_0^1 k_{22}(r,s) f_2(r)\,\mathrm{d}r = -\frac{\kappa+1}{2G}q(s). \end{aligned} \tag{18}$$

The unknown function $f_i(r)$ $(i = 1, 2)$ is approximated by the product of the fundamental dislocation density function $w_i(r)$ $(i = 1, 2)$ and Chebyshev polynomial $T_n(r)$. Equation (9) is applied to the first term of (18) and the second, the third and fourth terms of (18) are integrated by using numerical integral. Then, (18) becomes the following set of 2N linear equations:

$$\begin{aligned} &\sum_{n=1}^{N} [a_n\{\pi U_{n-1}(s) + A_n(s)\} + b_n B_n(s)] = -\pi p(s), \\ &\sum_{n=1}^{N} [a_n C_n(s) + b_n\{\pi U_{n-1}(s) + D_n(s)\}] = -\pi q(s), \end{aligned} \tag{19}$$

where

$$\begin{aligned} A_n(s) &= -\int_{-1}^{0} \frac{T_n(r)}{(r-s)\sqrt{1-r^2}}\,\mathrm{d}r + \int_0^1 k_{11}(r,s)\frac{T_n(r)}{\sqrt{1-r^2}}\,\mathrm{d}r, \\ B_n(s) &= \int_0^1 k_{12}(r,s)\frac{T_n(r)}{\sqrt{1-r^2}}\,\mathrm{d}r, \\ C_n(s) &= \int_0^1 k_{21}(r,s)\frac{T_n(r)}{\sqrt{1-r^2}}\,\mathrm{d}r, \\ D_n(s) &= -\int_{-1}^{0} \frac{T_n(r)}{(r-s)\sqrt{1-r^2}}\,\mathrm{d}r + \int_0^1 k_{22}(r,s)\frac{T_n(r)}{\sqrt{1-r^2}}\,\mathrm{d}r. \end{aligned} \tag{20}$$

The unknown coefficients a_n, b_n are determined from (19). The convenient set of collocation points is given by

$$s = \cos\left(\frac{2j}{2N-1}\tfrac{1}{2}\pi\right), \quad j = 1, 2, \ldots N, \quad (0 < s < 1). \tag{21}$$

The stress intensity factors can be calculated from

$$K_{\mathrm{I}} = F_{\mathrm{I}}(1)\sqrt{\pi a}, \quad K_{\mathrm{II}} = F_{\mathrm{II}}(1)\sqrt{\pi a}. \tag{22}$$

2.3. Numerical solution for notch problem

We consider a semi-infinite plate with a semi-elliptical notch as shown in Fig. 1 to explain the numerical solution of stress concentration problems. The problem can be solved by using the stress field at an arbitrary point ($x = a\cos\theta, y = b\sin\theta$) when a point force acts at another point ($\xi = a\cos\phi, \eta = b\sin\phi$) in a semi-infinite plate, on the basis of the principle of the super-position [9, 10]. This problem may be reduced to the following integral equations, where the body force densities distributed along the prospective boundary of the notch in the x, y directions $\rho_x^*(\phi)$, $\rho_y^*(\phi)$ are to be unknown functions

$$\begin{aligned} &-\tfrac{1}{2}\{\rho_x^*(\theta)\cos\theta_0 + \rho_y^*(\theta)\sin\theta_0\} \\ &\quad + \int_0^{\pi} K_{nn}^{F_x}(\phi,\theta)\rho_x^*(\phi)\,\mathrm{d}s + \int_0^{\pi} K_{nn}^{F_y}(\phi,\theta)\rho_y^*(\phi)\,\mathrm{d}s = -\sigma^{\infty}\sin^2\theta_0, \\ &-\tfrac{1}{2}\{\rho_x^*(\theta)\sin\theta_0 + \rho_y^*(\theta)\cos\theta_0\} \\ &\quad + \int_0^{\pi} K_{nt}^{F_x}(\phi,\theta)\rho_x^*(\phi)\,\mathrm{d}s + \int_0^{\pi} K_{nt}^{F_y}(\phi,\theta)\rho_y^*(\phi)\,\mathrm{d}s = -\sigma^{\infty}\sin\theta_0\cos\theta_0, \end{aligned} \tag{23}$$

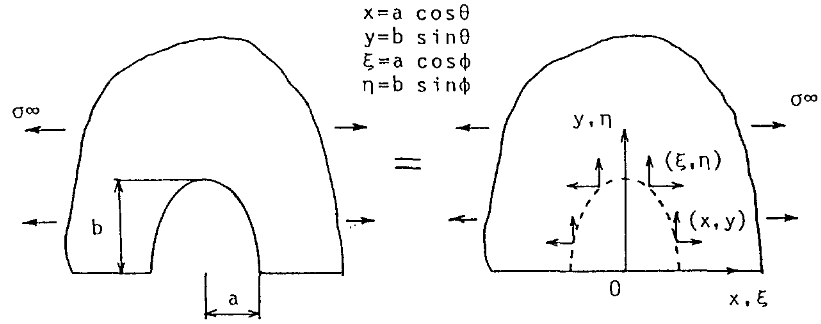

Fig. 1. Semi-elliptical notch in a semi-infinite plate.

where

$$-\,\mathrm{d}\xi = a\sin\phi\,\mathrm{d}\phi,\quad \mathrm{d}\eta = b\cos\phi\,\mathrm{d}\phi,\quad \mathrm{d}s = \sqrt{a^2\sin^2\phi + b^2\cos^2\phi}\,\mathrm{d}\phi,$$

$$\theta_0 = \arctan(b^2y/a^2x).$$

θ_0 is the angle between x-axis and normal direction of the notch at the point (x, y).

Equations (23) are virtually the boundary conditions on the imaginary boundary; that is, $\sigma_n = 0$, $\tau_{nt} = 0$. The first terms of (23) represent the stresses due to the body force distributed on the $\ominus$ boundary. The $\ominus$ boundary means the imaginary boundary composed of the internal points that are infinitesimally apart from the initial boundary [9]. Taking $K_{nn}^{F_x}(\phi, \theta)$ for example, the notation means the normal stress σ_n induced at the point (x, y) when the body force with unit density in the x-direction is acting at the infinitesimal arc length $\mathrm{d}s = \sqrt{(\mathrm{d}\xi)^2 + (\mathrm{d}\eta)^2}$. These equations include the singular terms having the singularity of the form $1/\sin\{(\theta - \phi)/2\}$ at $\theta = \phi$ [11], in this case the integrations should be interpreted as the meaning of Cauchy's principal values.

The unknown functions of the singular integral equations (23) $\rho_x^*(\phi)$, $\rho_y^*(\phi)$ are defined by the following equations, where the components of the resultant of the body force in the x, y directions acting on the infinitesimal arc length $\mathrm{d}s$ are $\mathrm{d}F_\xi$, $\mathrm{d}F_\eta$, respectively

$$\rho_x^*(\phi) = \frac{\mathrm{d}F_\xi}{\mathrm{d}s},\quad \rho_y^*(\phi) = \frac{\mathrm{d}F_\eta}{\mathrm{d}s}. \tag{24}$$

In the numerical solution of the singular integral equations (23), the unknown functions $\rho_x^*(\phi)$, $\rho_y^*(\phi)$ are approximated by the products of the weight functions $\rho_x(\phi)$, $\rho_y(\phi)$ and the fundamental density functions n_x, n_y [11].

$$\rho_x^*(\phi) = \frac{\mathrm{d}F_\xi}{\mathrm{d}s} = \frac{\mathrm{d}F_\xi}{\mathrm{d}\eta}n_x = \rho_x(\phi)\,n_x,$$

$$\rho_y^*(\phi) = -\frac{\mathrm{d}F_\eta}{\mathrm{d}s} = -\frac{\mathrm{d}F_\eta}{\mathrm{d}\xi}n_y = \rho_y(\phi)\,n_y, \tag{25}$$

where n_x and n_y are the x- and y-component of the unit vector in the normal direction at the point (x, y), respectively

$$n_x = \frac{\mathrm{d}\eta}{\mathrm{d}s} = \cos\theta_0 = \frac{b\cos\phi}{\sqrt{a^2\sin^2\phi + b^2\cos^2\phi}},\quad n_y = -\frac{\mathrm{d}\xi}{\mathrm{d}s} = \sin\theta_0 = \frac{a\sin\phi}{\sqrt{a^2\sin^2\phi + b^2\cos^2\phi}}. \tag{26}$$

In the previous analysis of the body force method, the imaginary notch boundary has divided into M equal intervals and the continuously varying unknown functions $\rho_x(\phi)$, $\rho_y(\phi)$ have been approximated by the stepped functions which take constant value in each interval. While in this paper, we use polynomials to approximate the weight functions as continuous functions. Now, from the symmetry of the problem we use following expressions

$$\rho_x(\phi) = \sum_{n=1}^{M} a_n t_n(\phi), \quad \rho_y(\phi) = \sum_{n=1}^{M} b_n t_n(\phi), \tag{27}$$

$$t_n(\phi) = (\tfrac{1}{2}\pi - \phi)^{2(n-1)}. \tag{28}$$

Using the approximation method mentioned above, we obtain the following system of linear equations for the determination of the coefficients a_n and b_n

$$\begin{aligned} &\sum_{n=1}^{M} (a_n A_n + b_n B_n) = -\sigma^\infty \sin^2\theta_0, \\ &\sum_{n=1}^{M} (a_n C_n + b_n D_n) = -\sigma^\infty \sin\theta_0 \cos\theta_0, \end{aligned} \tag{29}$$

$$\begin{aligned} A_n &= -\tfrac{1}{2}t_n(\theta)\cos^2\theta_0 + \int_0^\pi K_{nn}^{F_x}(\phi,\theta) b \cos\phi\, t_n(\phi)\,\mathrm{d}\phi, \\ B_n &= -\tfrac{1}{2}t_n(\theta)\sin^2\theta_0 + \int_0^\pi K_{nn}^{F_y}(\phi,\theta) a \sin\phi\, t_n(\phi)\,\mathrm{d}\phi, \\ C_n &= \tfrac{1}{2}t_n(\theta)\sin\theta_0\cos\theta_0 + \int_0^\pi K_{nt}^{F_x}(\phi,\theta) b \cos\phi\, t_n(\phi)\,\mathrm{d}\phi, \\ D_n &= -\tfrac{1}{2}t_n(\theta)\sin\theta_0\cos\theta_0 + \int_0^\pi K_{nt}^{F_y}(\phi,\theta) a \sin\phi\, t_n(\phi)\,\mathrm{d}\phi. \end{aligned} \tag{30}$$

The stresses at an arbitrary point are represented by a linear combination of the coefficients a_n, b_n and the influence coefficients correspond to A_n, B_n, C_n and D_n.

Using above numerical solution we will obtain the stress concentration factors and the stress distribution along the notch boundary in the semi-infinite plate.

3. Numerical results and discussion

3.1. Cruciform crack in an infinite plate

As an application of the present method mentioned above, the problem of a symmetric cruciform crack whose length of each branch is 'a' in an elastic infinite plate under constant tensile stress σ along all its four branches is treated (Fig. 2). The singular integral equation of this problem is shown by the following equation

$$\int_{-a}^{a} \frac{P(\xi)}{\xi - x}\,\mathrm{d}\xi + \int_{-a}^{a} \frac{\xi(\xi^2 - x^2)}{(\xi^2 + x^2)^3} P(\xi)\,\mathrm{d}\xi = -\pi\frac{\kappa+1}{2G}\sigma. \tag{31}$$

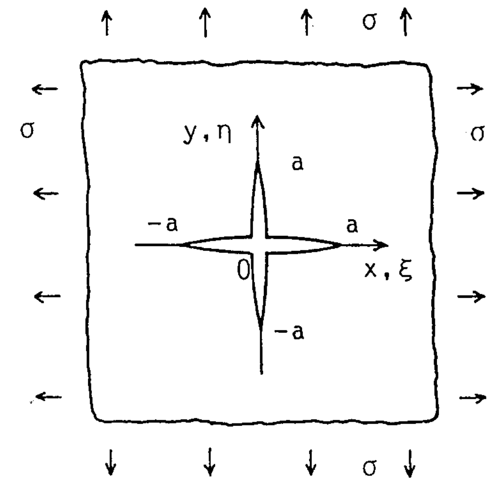

Fig. 2. Cruciform crack in an infinite plate.

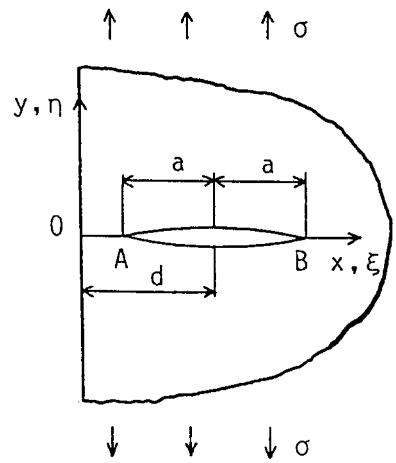

Fig. 3. Internal crack in a semi-infinite plate.

In Table 1 the convergency of the stress intensity factors of symmetric cruciform crack is shown to be compared with other numerical results [3, 4]. Here N is the number of collocation points in the range of $-a \leqslant x \leqslant a$. The present results show better convergency than the quadrature method of Gauss-Chebyshev and Lobatto-Chebyshev and worse convergency than the results of Boiko et al. However, the stress intensity factor obtained by the present method when $N/2 = 15$ coincides with Boiko's results in the 4 digits.

3.2. *Internal crack in a semi-infinite plate*

As another application of the present method, the problem of an internal crack whose length is $2a$ in an elastic semi-infinite plate under constant tensile stress σ is treated (Fig. 3). The singular

Table 1. Dimensionless stress intensity factors at the tip of a cruciform crack shown in Fig. 2 $[K_I/(\sigma\sqrt{\pi a})]$

N	Present analysis	Boiko-Karpenko [4]	Lobatto-Chebyshev Method [3]	Gauss-Chebyshev Method [3]
2	0.90281	0.86412	0.83658	0.94445
3	0.85374	0.86428	0.85970	0.83635
4	0.86687	0.86379	0.86387	0.83882
5	0.86168	0.86365	0.86449	0.86289
6	0.86341	0.86359	0.86441	0.86381
7	0.86296	0.86356	0.86424	0.86528
8	0.86318	0.86356	0.86408	0.86282
9	0.86328	0.86353	0.86396	0.86503
10	0.86325	0.86356	0.86387	0.86283
12	0.86334			
15	0.86348			
18	0.86351			
21	0.86352			
25	0.86343			
30	0.86343			
35	0.86354			

integral equation of this problem is shown by the following equation

$$\int_{d-a}^{d+a} \frac{P(\xi)}{\xi - x} \mathrm{d}\xi + \int_{d-a}^{d+a} \frac{x^2 + 4\xi x - \xi^2}{(\xi + x)^3} P(\xi)\,\mathrm{d}\xi = -\pi \frac{\kappa + 1}{2G} \sigma \tag{32}$$

In Table 2 (a), (b), (c), (d) the convergency of the stress intensity factors of internal crack is compared with Fujimoto's numerical results [5]. Here N is the number of collocation points in the range of $-a \leqslant x \leqslant a$. The present results show worse convergency than Fujimoto's results. However, with an increase of N the present results coincide with Fujimoto's results in the 7 digits completely.

3.3. *Edge crack in a semi-infinite plate*

As an application of the present method for the edge crack, the problem of an edge crack whose length is 'a' in a semi-infinite plate under constant tensile stress σ is treated (Fig. 4). This singular

Table 2. Dimensionless stress intensity factors at the tip of an internal crack shown in Fig. 3 $[K_\mathrm{I}/(\sigma\sqrt{\pi a})]$. (a) In case of $a/d = 0.5$. (b) In case of $a/d = 0.8$. (c) In case of $a/d = 0.9$. (d) In case of $a/d = 0.99$

(a) $a/d = 0.5$

	Present analysis		Fujimoto [5]	
N	$F_\mathrm{I}(A)$	$F_\mathrm{I}(B)$	$F_\mathrm{I}(A)$	$F_\mathrm{I}(B)$
1	1.089895	1.051646	1.094767	1.054415
2	1.091654	1.053985	1.091304	1.053898
3	1.091332	1.053914	1.091304	1.053904
4	1.091305	1.053904	1.091304	1.053904
5	1.091304	1.053904	1.091304	1.053904
6	1.091304	1.053904	1.091304	1.053904
7	1.091304	1.053904	1.091304	1.053904
8	1.091304	1.053904	1.091304	1.053904
9	1.091304	1.053904	1.091304	1.053904
10	1.091304	1.053904	1.091304	1.053904

(b) $a/d = 0.8$

	Present analysis		Fujimoto [5]	
N	$F_\mathrm{I}(A)$	$F_\mathrm{I}(B)$	$F_\mathrm{I}(A)$	$F_\mathrm{I}(B)$
1	1.354188	1.123180	1.491856	1.171283
2	1.402175	1.146014	1.389341	1.145685
3	1.392623	1.146908	1.387476	1.146380
4	1.388719	1.146573	1.387524	1.146416
5	1.387771	1.146452	1.387528	1.146417
6	1.387574	1.146424	1.387528	1.146417
7	1.387536	1.146418	1.387528	1.146417
8	1.387529	1.146417	1.387528	1.146417
9	1.387528	1.146417	1.387528	1.146417
10	1.387528	1.146417	1.387528	1.146417

Table 2.—Contd.

(c) $a/d = 0.9$				
	Present analysis		Fujimoto [5]	
N	$F_{\mathrm{I}}(A)$	$F_{\mathrm{I}}(B)$	$F_{\mathrm{I}}(A)$	$F_{\mathrm{I}}(B)$
1	1.553727	1.153680	2.069667	1.300961
2	1.745955	1.198726	1.742502	1.202468
3	1.738335	1.204325	1.708220	1.203254
4	1.721242	1.204419	1.707451	1.203730
5	1.712807	1.204100	1.707622	1.203791
6	1.709469	1.203918	1.707653	1.203797
7	1.708266	1.203841	1.707656	1.203797
8	1.707855	1.203812	1.707656	1.203798
9	1.707720	1.203802	1.707656	1.203798
10	1.707676	1.203799	1.707656	1.203798
11	1.707662	1.203798		
12	1.707658	1.203798		
13	1.707656	1.203798		
14	1.707656	1.203798		

(d) $a/d = 0.99$				
	Present analysis		Fujimoto [5]	
N	$F_{\mathrm{I}}(A)$	$F_{\mathrm{I}}(B)$	$F_{\mathrm{I}}(A)$	$F_{\mathrm{I}}(B)$
3	3.229821	1.307982	4.895297	1.372572
6	3.786204	1.328642	3.714837	1.328830
9	3.756009	1.330088	3.626008	1.329372
12	3.689253	1.330034	3.625948	1.329740
15	3.653149	1.329904	3.627061	1.329756
18	3.637370	1.329826	3.627272	1.329762
21	3.631059	1.329788	3.627299	1.329763
24	3.628662	1.329773	3.627301	1.329763
27	3.627783	1.329764	3.627301	1.329763
30	3.627469	1.329764	3.627301	1.329763
33	3.627359	1.329764	3.627301	1.329763
36	3.627320	1.329763		
39	3.627308	1.329763		
42	3.627304	1.329763		
45	3.627302	1.329763		
48	3.627301	1.329763		
50	3.627301	1.329763		

integral equation of the problem is shown by the following equation

$$\int_0^a \frac{P(\xi)}{\xi - x}\,\mathrm{d}\xi + \int_0^a \frac{x^2 + 4\xi x - \xi^2}{(\xi + x)^3} P(\xi)\,\mathrm{d}\xi = -\pi\frac{\kappa + 1}{2G}\sigma. \tag{33}$$

In Table 3 the convergency of the stress intensity factors of edge crack is compared with Boiko and Kerpenko's numerical results [4]. Here N is number of collocation points in the range of $0 \leqslant x \leqslant a$. In an edge crack problem, results of other researchers show worse convergency compared with internal crack problems. On the other hand, the stress intensity factor obtained by the present method coincides with Koiter's exact solution [12, 13] in the 7 digits when

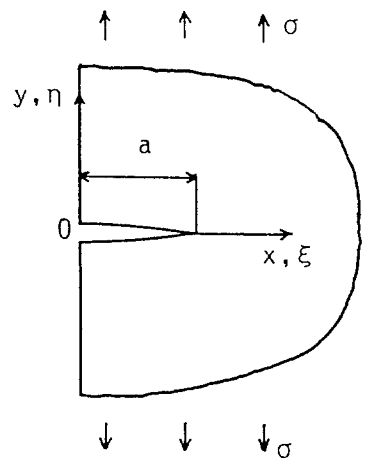

Fig. 4. Edge crack in a semi-infinite plate.

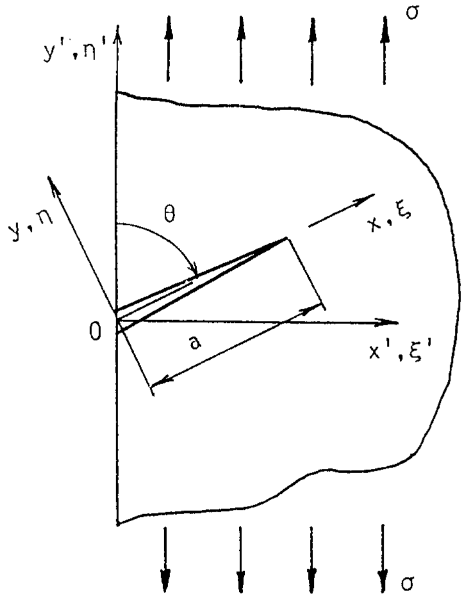

Fig. 5. Oblique edge crack in a semi-infinite plate.

Table 3. Dimensionless stress intensity factors at the tip of an edge crack shown in Fig. 4 $[K_{\mathrm{I}}/(\sigma\sqrt{\pi a})]$

N	Present analysis	Boiko [4]		Kerpenko [4]
10	1.121853	1.12379	1.11801	1.1194
20	1.121537	1.12212	1.12054	1.1209
30	1.121524	1.12182	1.12103	1.113
40	1.121521	1.12167	1.12147	1.1214
50	1.121521	1.12148	1.12121	1.1214
Koiter	1.121522			

$N = 30$. The present results have almost the same accuracy as the results of hypersingular integral equation shown in the previous papers [7, 8].

3.4. *Oblique edge crack in a semi-infinite plate*

As another application of the present method, the problem of an oblique edge crack whose length is 'a' in an elastic semi-infinite plate under constant tensile stress σ is treated (Fig. 5). The singular integral equations of this problem are shown by the following equations

$$\frac{2G}{\pi(\kappa+1)}\int_0^a \frac{P_1(\xi)}{\xi - x}\,\mathrm{d}\xi + \int_0^a K_{11}(\xi, x)P_1(\xi)\,\mathrm{d}\xi + \int_0^a K_{12}(\xi, x)P_2(\xi)\,\mathrm{d}\xi = -\,p(x),$$

$$\frac{2G}{\pi(\kappa+1)}\int_0^a \frac{P_2(\xi)}{\xi - x}\,\mathrm{d}\xi + \int_0^a K_{21}(\xi, x)P_1(\xi)\,\mathrm{d}\xi + \int_0^a K_{22}(\xi, x)P_2(\xi)\,\mathrm{d}\xi = -\,q(x), \tag{34}$$

$$p(x) = \sigma \sin^2\theta, \quad q(x) = \sigma \sin\theta\cos\theta,$$

where $K_{ij}(\xi, x)$ $(i, j = 1, 2)$ is a function known to satisfy the boundary condition except at the crack surface and expressed by the following equations

$$\begin{aligned} K_{11}(\xi, x) &= \sigma_{y'}^{By} \sin^2\theta + \sigma_{x'}^{By} \cos^2\theta - 2\tau_{x'y'}^{By} \sin\theta\cos\theta, \\ K_{12}(\xi, x) &= \sigma_{y'}^{Bx} \sin^2\theta + \sigma_{x'}^{Bx} \cos^2\theta - 2\tau_{x'y'}^{Bx} \sin\theta\cos\theta, \\ K_{21}(\xi, x) &= (\sigma_{y'}^{By} - \sigma_{x'}^{By}) \sin\theta\cos\theta + \tau_{x'y'}^{By}(\sin^2\theta - \cos^2\theta), \\ K_{22}(\xi, x) &= (\sigma_{y'}^{Bx} - \sigma_{x'}^{Bx}) \sin\theta\cos\theta + \tau_{x'y'}^{Bx}(\sin^2\theta - \cos^2\theta), \end{aligned} \tag{35}$$

$$\begin{aligned} \sigma_{x'}^{Bx}|_{Bx=1} &= \sigma_{x'}^{By'}|_{By'=1} \cos\theta - \sigma_{x'}^{Bx'}|_{Bx'=1} \sin\theta, \\ \sigma_{x'}^{By}|_{By=1} &= \sigma_{x'}^{By'}|_{By'=1} \sin\theta + \sigma_{x'}^{Bx'}|_{Bx'=1} \cos\theta. \end{aligned} \tag{36}$$

$\sigma_{y'}^{Bx}$, $\tau_{x'y'}^{Bx}$, $\sigma_{y'}^{By}$ and $\tau_{x'y'}^{By}$ can be expressed by the similar manner of Eqn. (36).

Taking σ_{x}^{Bx} for example, the notation means the normal stress in the x-direction induced at the point (x, y) to eliminate the stresses σ_x and τ_{xy} induced at the free edge $(x' = 0)$ when the edge dislocation with Burgers vector Bx which is parallel to the x-direction exists at the point (ξ, η) in the semi-infinite plate. $\sigma_{x'}^{By'}$ etc. in (36) are expressed by the following expression

$$\begin{aligned} \sigma_{x'}^{Bx'} &= C[-A^5 - 4(n^2 - n + 1)A^3 - 3n^2(n^2 + 4n - 4)A]Bx', \\ \sigma_{y'}^{Bx'} &= C[-A^5 - 4(2n^2 - n - 1)A^3 - n^2(7n^2 - 20n + 12)A]Bx', \\ \tau_{x'y'}^{Bx'} &= C[-(n - 2)A^4 + 12n(n - 1)A^2 - n^3(n^2 - 6n + 4)]Bx', \\ \sigma_{x'}^{By'} &= C[(n - 2)A^4 + 12n(n - 1)A^2 - n^3(n^2 + 2n - 4)]By', \\ \sigma_{y'}^{By'} &= C[(5n - 2)A^4 + 4n(n^2 - 3n + 3)A^2 - n^3(n^2 - 6n + 4]By', \\ \tau_{x'y'}^{By'} &= C[A^5 - 4(n - 1)A^3 - n^2(n^2 - 12n + 12)A]By', \end{aligned} \tag{37}$$

where A, n and C are shown by (38).

$$A = \frac{\eta' - y'}{x'}, \quad n = \frac{\xi' - x'}{x'}, \quad C = \frac{2G}{\pi(\kappa + 1)} \cdot \frac{1}{x'(A^2 + n^2)^3}. \tag{38}$$

This problem has been solved by the hypersingular integral equation method where the discontinuity or body force doublet densities $[P_1^*(\xi), P_2^*(\xi)]$ which have stronger singularity than the dislocation are to be unknown functions [7, 8]. The singular integral equations are shown by the following equations

$$\int_0^a \frac{P_1^*(\xi)}{(\xi - x)^2} \, d\xi + \int_0^a K_{11}^*(\xi, x) P_1(\xi) \, d\xi + \int_0^a K_{12}^*(\xi, x) P_2(\xi) = p^*(x),$$

$$\int_0^a \frac{P_2^*(\xi)}{(\xi - x)^2} d\xi + \int_0^a K_{21}^*(\xi, x) P_1(\xi) d\xi + \int_0^a K_{22}^*(\xi, x) P_2(\xi) d\xi = -q^*(x),$$

$$p^*(x) = -\pi \frac{(\kappa+1)^2}{2(\kappa-1)} \sigma \sin^2\theta, \quad q^*(x) = -\pi \frac{\kappa+1}{2} \sigma \sin\theta \cos\theta, \tag{39}$$

where $\neq$ is interpreted in the Hadamard sense by retaining the finite part of the divergent integral and the kernel $K_{ij}^*(\xi, x)$ $(i, j = 1, 2)$ is a function known to satisfy the boundary condition except at the crack surface. These integral equations have been solved using the same approximation, namely, by the product of the fundamental density function and Chebyshev polynomials. In Table 4 the convergency of the stress intensity factors of oblique edge crack are shown and compared with the numerical results of the hypersingular integral equation method in the previous papers [7, 8]. Here N is the number of collocation points in the range of $0 \leqslant x \leqslant a$. It is found that in the case of $\theta \geqslant 15°$ both results have almost the same accuracy.

3.5. *Semi-elliptical notch in a semi-infinite plate*

Figure 6 (a), (b) shows the comparison of the approximation of the unknown functions between the polynomials and the stepped functions for $b/a = 1$, 2. In the present analysis using the polynomials, the expression of $M = 12$ and the one of $M = 24$ almost coincide with each other and therefore they seem to express the unknown functions ρ_x and ρ_y very accurately. On the other hand, when we use the stepped functions, both expressions of $M = 12$ and $M = 24$ do not coincide with the present analysis especially near the free edge ($\theta < 10°$).

Table 4. Dimensionless stress intensity factors at the tip of an oblique edge crack in Fig. 5 $[K_I/(\sigma\sqrt{\pi a}), K_{II}/(\sigma\sqrt{\pi a})]$

θ deg.	N	Present analysis F_I	Present analysis F_{II}	HIEM [7, 8] F_I	HIEM [7, 8] F_{II}
45°	5	0.70403	0.36557	0.70403	0.36557
	10	0.70500	0.36455	0.70449	0.36455
	15	0.70488	0.36446	0.70488	0.36446
	20	0.70489	0.36448	0.70489	0.36447
	25	0.70490	0.36448	0.70490	0.36448
30°	10	0.46256	0.35388	0.46260	0.33590
	15	0.46254	0.33620	0.46257	0.33620
	20	0.46252	0.33619	0.46254	0.33619
	24	0.46250	0.33617	0.46250	0.33617
	30	0.46247	0.33616	0.46247	0.33616
15°	20	0.23197	0.22618	0.23225	0.22637
	25	0.23180	0.22616	0.23184	0.22617
	30	0.23188	0.22621	0.23182	0.22616
	35	0.23180	0.22614	0.23181	0.22615
	40	0.23174	0.22616	0.23180	0.22614
10°	30	0.18916	0.18916	0.16125	0.17333
	35	0.16108	0.17408	0.16207	0.17347
	40	0.16236	0.17337	0.16206	0.17346
	45	0.16782	0.17054	0.16205	0.17345
	50	0.16155	0.17428	0.16205	0.17345

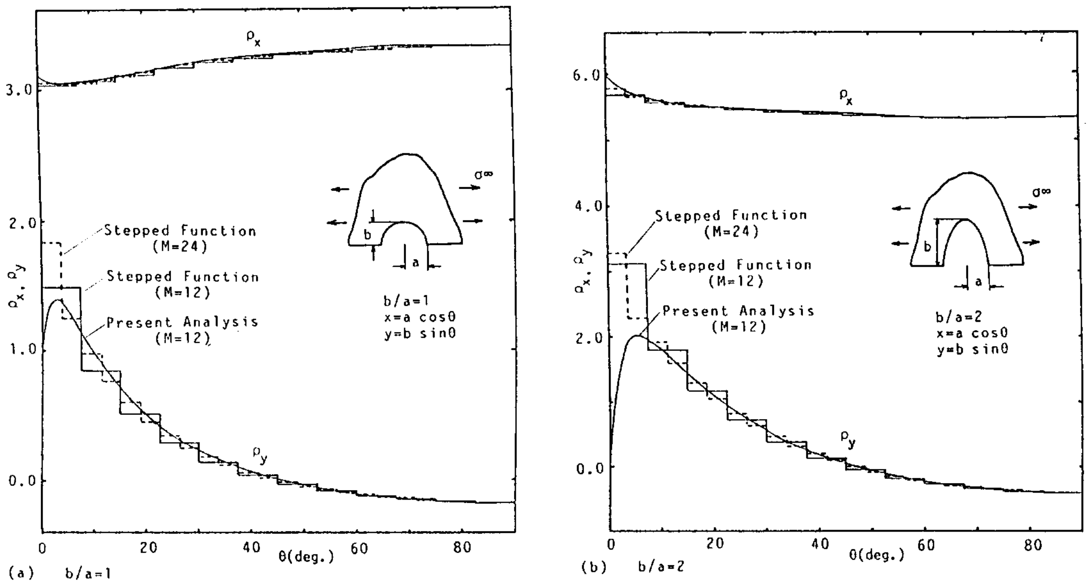

Fig. 6. Comparison of the approximation of the unknown functions between the polynomials and the stepped function. (a) In case of $b/a = 1$. (b) In case of $b/a = 2$.

In Table 5 (a), (b), (c) the convergency of the stress concentration factors is compared with the previous body force method using stepped functions. Here, we consider the rapid change of the density of the body force near the free edge, we put $M1$ collocation points in $0° \leqslant \theta \leqslant 10°$ and $M2$ in $10° \leqslant \theta \leqslant 90°$. Therefore, $M = M1 + M2$ is total collocation point number in

Table 5. Convergency of the stress concentration factors (Comparison between the polynomials and the stepped function). (a) In case of $b/a = 1$. (b) In case of $b/a = 2$. (c) In case of $b/a = 10$

(a) $b/a = 1$

Present analysis		B.F.M.	
M	K_t	M	K_t
4	3.056586	8	3.052064
6	3.061805	12	3.056805
8	3.064102	24	3.061290
10	3.064920	32	3.062307
12	3.065215	48	3.063353
14	3.065321	$\infty(48-32)$	3.0654
		[14]	3.0653

(b) $b/a = 2$

Present analysis		B.F.M.	
M	K_t	M	K_t
4	5.199307	8	5.178407
6	5.213694	12	5.193873
8	5.218326	24	5.207968
10	5.219638	32	5.211044
12	5.220068	48	5.214306
14	5.220230	$\infty(48-32)$	5.2208
		[14]	5.2204

(c) $b/a = 10$			
Present analysis		B.F.M.	
M	K_t	M	K_t
4	22.90348	8	22.50020
6	23.02375	12	22.64869
8	23.00240	24	22.81734
10	22.99309	32	22.85534
12	22.99903	48	22.90320
14	23.00849	$\infty(48-32)$	22.999
		[14]	23.000

Table 6. Stress along the notch boundary at the mid-point of collocation points ($b/a = 1$, $M1 = 4$, $M2 = 8$ in Fig. 1)

θ (deg.)	σ_θ	σ_r	$\tau_{r\theta}$
1	−0.0012	0.00042	−0.00040
3	−0.0108	0.00003	0.00004
5	−0.0266	−0.00001	−0.00001
7	−0.0398	0.00001	0.00001
13.5	−0.0326	−0.00025	−0.00037
23.4	0.1814	0.00012	0.00015
32.3	0.5499	−0.00006	−0.00006
41.2	1.0332	0.00003	0.00001
50.0	1.5621	−0.00002	0.00000
58.9	2.0854	0.00001	0.00000
67.8	2.5376	−0.00001	0.00000
76.7	2.8689	0.00002	0.00000

$0 \leqslant \theta \leqslant \pi/2$. In Table 5, the symbol ∞ (48 − 32) designates the extrapolated value using the results of $M = 48$ and $M = 32$. The stress concentration factor by the present method $M = 12$ coincides with the results of Chen et al. [14] in the 5 digits. The present results show better convergency than the results using stepped functions which need the extrapolation.

In order to investigate the satisfaction of the boundary conditions ($\sigma_r = 0, \tau_{r\theta} = 0$), Table 6 shows the stress distribution along the semi-circular notch boundary at the mid-point of the collocation points. Here, $M1 = 4$, $M2 = 8$, and the total collocation point number M is 12. The values of σ_r and $\tau_{r\theta}$ which should be 0 along the boundary are less than 10^{-3} even for $M = 12$. Therefore, in the present analysis, it is found that the boundary requirements can be highly satisfied anywhere along the boundary.

4. Conclusion

In this paper, the numerical solution of the Cauchy-type singular integral equations based on the continuously distributed dislocation method in crack problems and the body force method in notch problems was investigated. In the numerical solution, the unknown functions are approximated by the product of the fundamental density functions and polynomials. The conclusions are summarized as follows:

(1) The stress intensity factors of a cruciform crack in an infinite plate and an internal crack in a semi-infinite plate were solved and compared with previous research. The present results

showed better convergency than the quadrature method of Gauss-Chebyshev and Lobatto-Chebyshev, and worse convergency than the results of Boiko and Fujimoto. However, with an increase of collocation points, the present results gave the same accuracy as the results of Boiko and Fujimoto.

(2) The stress intensity factors of an edge crack in semi-infinite plate were solved and compared with previous research. Other numerical methods could not give the solution with the same accuracy as the internal crack problem. However, the present results of an edge crack having the right angle to the free edge coincided with Koiter's exact solution in the 7 digits. Moreover, the oblique edge crack problem was found to be solved with almost the same accuracy as the solution of the hypersingular integral equation method.

(3) The stress concentration factors of a semi-elliptical notch in a semi-infinite plate were calculated. The present method gave more accurate results than the previous body force method where the stepped functions and the extrapolation method were used. And the present analysis could highly satisfy the boundary conditions and gave the exact stress distribution anywhere along the boundary.

(4) In the numerical solution of the Cauchy-type singular integral equation, an approximation of the unknown functions by the product of the fundamental density function and the polynomials was found to give good convergency of the numerical results for various kinds of notch and crack problems.

References

1. F. Erdogan and G.D. Gupta, *Quarterly of Applied Mathematics* 30 (1972) 525–534.
2. F. Erdogan, G.D. Gupta and T.S. Cook, in *Mechanics of Fracture*, G.C. Sih (ed.) Noordhoff International Publication, Leyden, 1 (1973) 368–425.
3. P.S. Theocaris and N.I. Ioakimidis, *Quarterly of Applied Mathematics* 35 (1977) 173–183.
4. A.V. Boiko and L.N. Karpenko, *International Journal of Fracture* 17–4 (1981) 381–388.
5. K. Fujimoto, *Transactions of the Japan Society of Mechanical Engineers* 56 A (1990) 1505–1510.
6. N.A. Noda, H. Umeki and F. Erdogan, *Transactions of the Japan Society of Mechanical Engineers* 55 A (1989) 2521–2526.
7. N.A. Noda, K. Oda and D.H. Chen, *Transactions of the Japan Society of Mechanical Engineers* 56 A (1990) 2405–2410.
8. N.A. Noda and K. Oda, *International Journal of Fracture* 58 (1992) 285–304.
9. H. Nisitani, *Journal of the Japan Society of Mechanical Engineers* 70 (1967) 627–635 [*Bulletin Japan Society of Mechanical Engineers* 11 (1968) 14–23].
10. N. Nisitani, in *Mechanics of Fracture*, G.C. Sih (ed.) Noordhoff International Publication, Leyden, 5 (1978) 1–68.
11. H. Nisitani and D.H. Chen, *The Body Force Method* (Taisekiryokuhou in Japanese) Baifukan Publication, Tokyo (1987).
12. W.T. Koiter, *Journal of Applied Mechanics* 32 (1965) 237.
13. A.C. Kaya and F. Erdogan, *Quarterly of Applied Mathematics* 45 (1987) 105–122.
14. D.H. Chen, H. Nisitani and K. Mori, *Transactions of the Japan Society of Mechanical Engineers* 55 A (1989) 948–953.